# A Spectrally Interrogated Polarimetric Optical Fiber Sensors for Current Measurement with Temperature Correction

Tinko A. Eftimov *, Georgi L. Dyankov, Petar Kolev, Veselin P. Vladev

Posted Date: 17 October 2023

doi: 10.20944/preprints202310.1020.v1

Keywords: magnetic field sensor; current sensor; temperature independent measuremenents; polarimetry; fibre optic sensors; spectral interrogation

*Article*

# A Spectrally Interrogated Polarimetric Optical Fiber Sensors for Current Measurement with Temperature Correction

**Tinko Eftimov [1,2,*], Georgi Dyankov [2,3], Petar Kolev [3] and Veselin Vladev [2,4]**

[1] Photonics Research Center, Université du Québec en Outaouais, Rue 101 St-Jean Bosco, Gatineau, Québec J8X 3G5, Canada; tinko.eftimov@uqo.ca
[2] Central Laboratory of Applied Physics, Bulgarian Academy of Sciences, 61 Sanct Peterburg Blvd., Plovdiv, Bulgaria
[3] Institute of Optical Materials and Technologies "Acad. J. Malinowski" (IOMT), Bulgarian Academy of Sciences (BAS), 109 "Acad. G. Bonchev" Str., 1113 Sofia, Bulgaria; ge.dyankov@iomt.bas.bg, p.kolev@iomt.bas.bg
[4] Department of Mathematics, Physics and Information Technologies, Faculty of Economics, Photonics Laboratory, University of Food Technologies, 26 Maritsa Blvd., Plovdiv, Bulgaria, v.p.vladev@abv.bg
* Correspondence: tinko.eftimov@uqo.ca

**Abstract:** We report on the study of the temperature dependence of the response of a BSO crystal based polarimetric current sensor with spectral interrogation. Two possible interrogation schemes are discussed. The spectral dependence of the optical rotation along the crystal caused by temperature and current changes has been investigated and approximate dependences for the sensitivities to current $S_I$ and temperature $S_T$ have been derived. A mixed term in the response with spectral interrogation has been revealed, the elimination of which is done by tracking wavelength shifts $\Delta\lambda_1$ and $\Delta\lambda_2$ of two distinct extrema in the polarimetric response. A temperature independent second degree equation for the current changes $\Delta I$ as a function of the spectral shifts has been derived and tested.

**Keywords:** magnetic field sensor; current sensor; temperature independent measuremenents; polarimetry; fibre optic sensors; spectral interrogation

## 1. Introduction

Faraday effect based electric current and/or magnetic field fiber optic sensors have been known, developed and commercialized [1] for quite some time for the purposes of the power industry [2] and special applications [3]. These sensors are based either on the Faraday effect in the fiber itself, or in bulk materials [4] which use optical fiber transducers such as fiber Bragg gratings (FBG), interferometers or refractometers [5–11] in combination with the magnetic field sensitive materials. These sensors are characterized by specific advantages / disadvantages and varying simplicity and complexity.

Among the simplest and most straightforward solutions are the polarimetric sensors using magneto-optical materials such as BSO ($Bi_{12}SiO_{20}$) and BGO ($Bi_4Ge_3O_{12}$) crystals because of their high Verdet constant and whose wavelength dependence has been accurately measured and well known [12,13]. The first polarimetric fiber optic sensor using BSO/BGO crystals [14,15], however operate at a single wavelength and detect amplitude changes of the polarimetric response. These crystals are also temperature dependent [16,17] which presents a limitation on the performance of the sensor. To account for temperature dependence, detection at two wavelengths has been proposed [18] or the temperature dependence of the BGO crystal has been taken into account [19]. The problem with the temperature dependence for the other types of the current sensors has been addressed in different ways depending on the interrogation scheme and the magneto-sensitive material by either

Preprints (www.preprints.org) | NOT PEER-REVIEWED | Posted: 17 October 2023 doi:10.20944/preprints202310.1020.v1



temperature compensation [18–23] or simultaneous magnetic field and temperature measurement in the case of magnetic field sensors with spectral interrogation [24–28].

We have recently shown [30,31] that the well-known fluorescence in BSO crystals [32] can be used to generate under ultraviolet or white LED excitation a broad spectrum which serves as broadband source for a polarimetric scheme with spectral interrogation. We have also reported [33] that the BSO crystal based polarimetric sensor exhibits a wavelength dependent temperature dependence.

In the present work we measure the optical activity of a BSO crystal at different temperatures, currents and wavelength and establish the spectral and temperature dependence of the intrinsic and magnetic field induced polarization rotation. We show that the spectrally interrogated polarimetric fiber optic current sensor using a white LED can be used eliminate the temperature dependence in the measurement of the electric current.

Section 2 presents the general experimental set-up, the principal of operation and the two possible interrogation techniques. Section 3 is devoted to the measurement of the spectral dependence of temperature-influenced optical activity from which we derive the spectral, temperature and current dependences of the sensitivities to current and temperature. To eliminate the temperature dependence we use the spectral shifts of two extrema of the polarimetric spectral response and derive an expression for the current changes. The performance of the current sensor is simulated numerically.

## 2. Principle of operation and experimental arrangement

### *2.1. Experimental set-up*

The experimental set-up in Figure 1 was used to generate a broad spectrum from 520 nm to 800 nm in the BSO crystal and to observe the spectral distribution of the polarimetric responses which is given by the expression [31]:

$$I = \frac{1}{4}\{1+\cos[2(\phi+\theta-\alpha)]\} \tag{1}$$

In (1) $\theta$ and $\alpha$ are the polarizer and analyzer orientations and

$$\phi = \Delta\beta L \tag{2}$$

is the accumulated phase along the circularly birefringent BSO crystal whose length is $L$ and $\Delta\beta = \beta_L - \beta_R$ is the propagation constant difference between the left and the right circularly polarized waves along the crystal. This difference is both wavelength and temperature dependent and is expressed as [31]:

$$\Delta\beta(\lambda,T) = \rho(\lambda,T) + V_B(\lambda,T)B \tag{3}$$

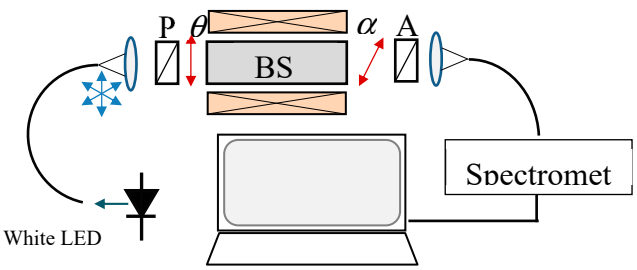


**Figure 1.** Polarimetric experimental arrangement.

In (3) $\rho$ (deg/mm) is the optical rotatory power of the crystal and the additional rotatory power $\rho_F = V_B B$ caused by the Faraday effect, $B$ being the magnetic field and $V_B$ the Verdet constant. The wavelength dependences of $\rho(\lambda)$ and $V_B(\lambda)$ is well known [12,13], both decrease with wavelength and

Preprints (www.preprints.org) | NOT PEER-REVIEWED | Posted: 17 October 2023 doi:10.20944/preprints202310.1020.v1



$V_B$ is proportional to $\rho$ [17]. Temperature dependences, however, have been insufficiently studied and further in the paper we present more detailed results. Inserting (3) and (2) into (1) we have for the wavelength and temperature dependent intensity $I(\lambda,T)$ [30,31].

$$I(\lambda,T)=\frac{1}{4}\{1+\cos[\Phi(B,T,\lambda)]\}=\frac{1}{4}\{1+\cos[2(\rho(\lambda,T)+V_B(\lambda,T)B)L+2(\theta-\alpha)]\} \quad (4)$$

$\Phi(B,T,\lambda)$ being the total phase in the polarimetric response. The typical spectral responses of a polarimetric sensor to changes of the polarizer/analyzer orientations and to current (magnetic field) are shown in Figure 2.

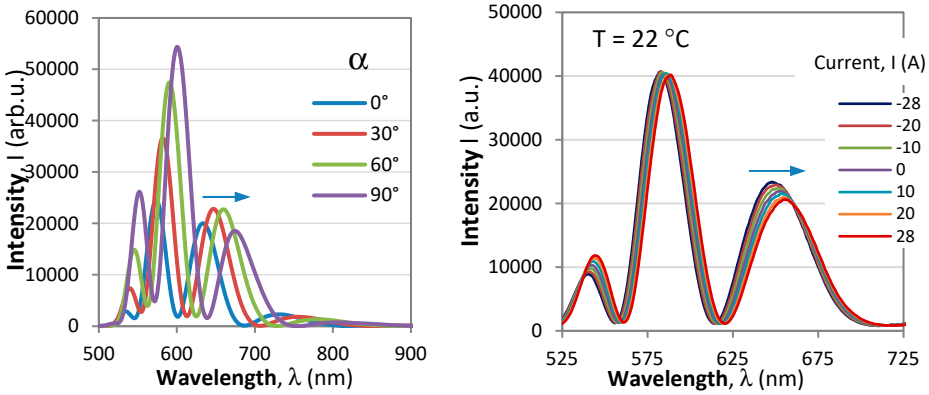


**Figure 2.** Spectral response of the polarimetric sensor response: a) as analyzer angle increases from 0°C to 90°C; b) as current in the coil increases form -28A to +28A.

The plots show that the particular position of the modulated pattern can be fine-tuned by changing the orientation of the analyzer / polarizer via the $\theta-\alpha$ term. The changes of the measurand (current / magnetic) field and for that matter of temperature lead to shifts of the polarimetric response as shown in Figure 2b)

*2.2. Principle of operation and sensitivities*

Unlike the single wavelength polarimetric arrangement [14] in which the intensity (4) is measured, in our arrangement we observe by a spectrometer the whole spectrum which exhibits an oscillatory response. Since both $\rho(\lambda)$ and $V_B(\lambda)$ decrease with wavelength the period of the wavelength dependent response $\Lambda$ (which is the free spectral range – FSR) increases with wavelength. As the angle between polarizer and analyzer can be varied, we can tune the phase $2(\theta-\alpha)$ and thus fix the position of the polarimetric response.

*2.3. Interrogation detection techniques*

There are two detection techniques that can be used to detect the changes in the polarimetric spectral response. In the first we track the wavelength position of a minimum $\lambda_m$ or a maximum $\lambda_M$, as the magnetic field/elecric current changes. Thus, the wavelegth shifts $\delta\lambda_M = \delta\lambda_M - \delta\lambda_{M,0}$ of a maximum and $\delta\lambda_m = \delta\lambda_m - \delta\lambda_{m,0}$ of a with respect to some wavelength positions at $I = 0$ A and $T = T_0$ are tracked. In the second, we observe the intensities that are $+\pi/2$ and $-\pi/2$ phase-shifted with respect to an extremum $I_M^+$ and $I_M^-$ for a maximum or $I_m^+$ and $I_m^-$ for a minimum and calculate the differences and the sums of intensities that are $\pi$-shifts with respect to one another: $\Delta_M = I_M^+ - I_M^-$, $\Sigma_M = I_M^+ + I_M^-$ and $\Delta_m = I_m^+ - I_m^-$, $\Sigma_m = I_m^+ + I_m^-$ and then calculate the normalized differences $N_M = \Delta_M / \Sigma_M$ and $N_m = \Delta_m / \Sigma_m$ which change with current/magnetic field and temperature.

Preprints (www.preprints.org) | NOT PEER-REVIEWED | Posted: 17 October 2023 doi:10.20944/preprints202310.1020.v1



2.3.1. Extrema wavelength shifts

In this case for a given magnetic field $B$ (or current $I$) and temperature $T$, the wavelengths $\lambda_{M,k}$ and $\lambda_{m,k}$ of the $k$-th maximum and minimum of the polarimetric response are those for which the phase $\Phi$ from (4) is:

$$\Phi_M(B,T,\lambda_{M,k}) = 2k\pi \quad \max \qquad \text{and} \qquad \Phi_m(B,T,\lambda_{m,k}) = (2k+1)\pi \quad \min \tag{5a}$$

and the phase change $\Delta\Phi$ is then

$$\Delta\Phi_k = \frac{\partial\Phi_k}{\partial\lambda}\Delta\lambda_k + \frac{\partial\Phi_k}{\partial I}\Delta I + \frac{\partial\Phi_k}{\partial T}\Delta T \tag{5b}$$

When we track the shifts $\Delta\lambda_k$ of an extremum (at $\lambda_{M,k}$ or $\lambda_{m,k}$) with respect to the position for $I = 0$ ($B = 0$) caused by changes of the magnetic field (or current) $\Delta B$ (or $\Delta I$) and of the temperature $\Delta T$, resultant phase change $\Delta\Phi$ of the $\Phi_M$ or $\Phi_m$ is zero because the condition (5a) for the tracked extremum remain the constant i.e. $\Phi_M = 2k\pi = const$ and $\Phi_M = 2k\pi = const$. The expression (5b) becomes null and solving with respect to $\Delta\lambda$ we obtain:

$$\Delta\lambda_k = \lambda_k - \lambda_{k,0} = -\left(\frac{\partial\Phi}{\partial B}\Big/\frac{\partial\Phi}{\partial\lambda}\right)\Delta B - \left(\frac{\partial\Phi}{\partial T}\Big/\frac{\partial\Phi}{\partial\lambda}\right)\Delta T = S_B\Delta B + S_T\Delta T \tag{6a}$$

where $S_B$ and $S_T$ are the sensitivities to magnetic field and temperature changes

$$S_B = \frac{\Delta\lambda_k}{\Delta B} \quad , \qquad S_T = \frac{\Delta\lambda_k}{\Delta T} \tag{6b}$$

In (5) and (6) $\lambda_k$ is either $\lambda_{M,k}$ or $\lambda_{m,k}$ as instantly tracked and $\Delta\lambda_k$ is the wavelength shift of the extremum from the initial value $\lambda_{k,0}$ for which $I = 0$ and $T = T_0$ This type of interrogation is illustrated in Figure 3a). Both the magnitude and the sign of the current / magnetic field can thus be measured. Figure 4a) shows the wavelength shifts of the extrema from the response in Figure 3a) which prove to be linear with wavelength, while Figure 4b) shows the correspondingly measure sensitivies which increase with wavelength [30,31].

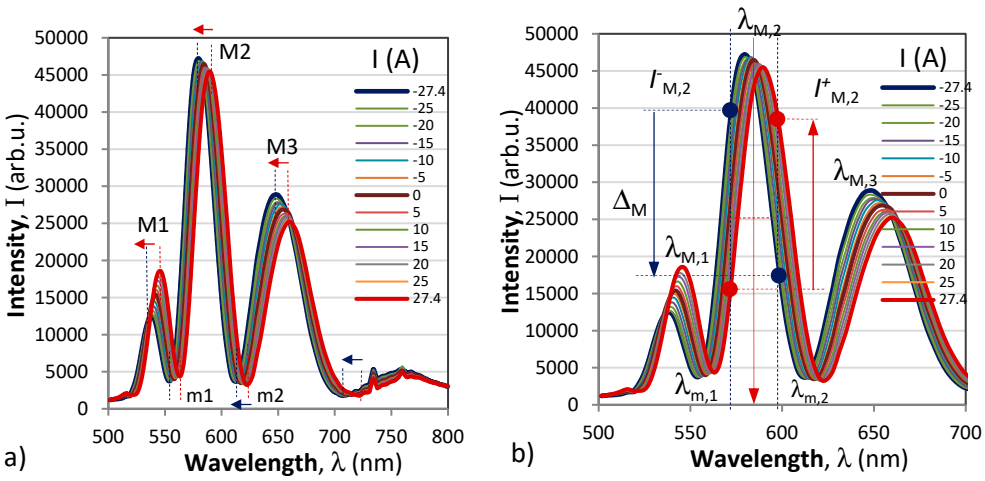


**Figure 3.** Interrogation techniques: a) extrema wavelength shift; b) π-shifted differential shift.

Preprints (www.preprints.org) | NOT PEER-REVIEWED | Posted: 17 October 2023 doi:10.20944/preprints202310.1020.v1



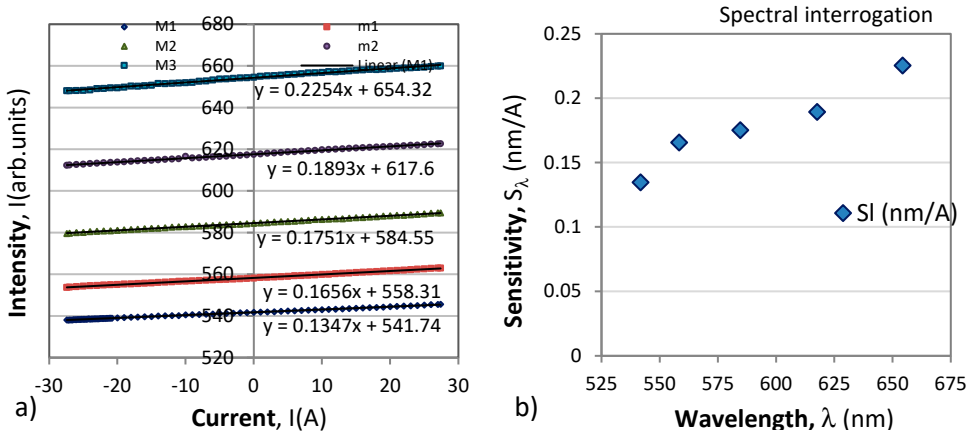


**Figure 4.** Spectral responses of the extrema shift interrogation technique: a) wavelength shifts of the the maxima $M_1$, $M_2$, $M_3$ and the minima $m_1$ and $m_2$, b) wavelength dependence of the sensitivities $S_I(\lambda)$.

2.3.2. $\pi$-shifted normalized differential response

In this case the intensities $I_k^{\ddot{}+}$ and $I_k^{\ddot{}-}$ of the polarimetric response around the *k*-th extremum ( $I_{M,k}^{\ddot{}\pm}$ and $I_{m,k}^{\ddot{}\pm}$ ) that are π-shifted to each other can be defined as:

$$I_k^{\ddot{}+} = I_0 \cos\left[2\phi_k + 2(\theta-\alpha) + \frac{\pi}{2}\right] \quad I_k^{\ddot{}-} = I_0 \cos\left[2\phi_k + 2(\theta-\alpha) - \frac{\pi}{2}\right] \tag{7}$$

The normalized differential responses around the *k*-th maximum or the minimum are defined as:

$$N_{M,k} = \frac{I_{M,k}^{\ddot{}+} - I_{M,k}^{\ddot{}-}}{I_{M,k}^{\ddot{}+} + I_{M,k}^{\ddot{}-}}, \qquad N_{m,k} = \frac{I_{m,k}^{\ddot{}+} - I_{m,k}^{\ddot{}-}}{I_{m,k}^{\ddot{}+} + I_{m,k}^{\ddot{}-}} \tag{8}$$

In the initial state $I_{M,k}^{\ddot{}+} = I_{m,k}^{\ddot{}-}$ , but when the polarimetric response shifts to the right the difference $\Delta = I_{M,k}^{\ddot{}+} - I_{M,k}^{\ddot{}-}$ becomes positive and vice versa as shown illustrated in Figure 3b) by the red and blue vertical arrows. Therefore, both the amplitude and the sign of the current/magnetic field can be detected. The sensitivities to magnetic field/current and to temperature are defined in this case as:

$$\Pi_{B,k} = 100\frac{\Delta N_k}{\Delta B} \text{ or } \Pi_{I,k} = 100\frac{\Delta N_k}{\Delta I}, \qquad \Pi_{T,k} = 100\frac{\Delta N_k}{\Delta T} \tag{9}$$

Figure 5 presents the responses of the normalized differential signals according to the π-shifted interrogation technique. As is seen the responses are with different sensitivites though not quite linear as those from Figure 4. The sensitivity in this case shows similar wavelength dependence as with the first interrogation method (Figure 4b).

Preprints (www.preprints.org) | NOT PEER-REVIEWED | Posted: 17 October 2023 doi:10.20944/preprints202310.1020.v1



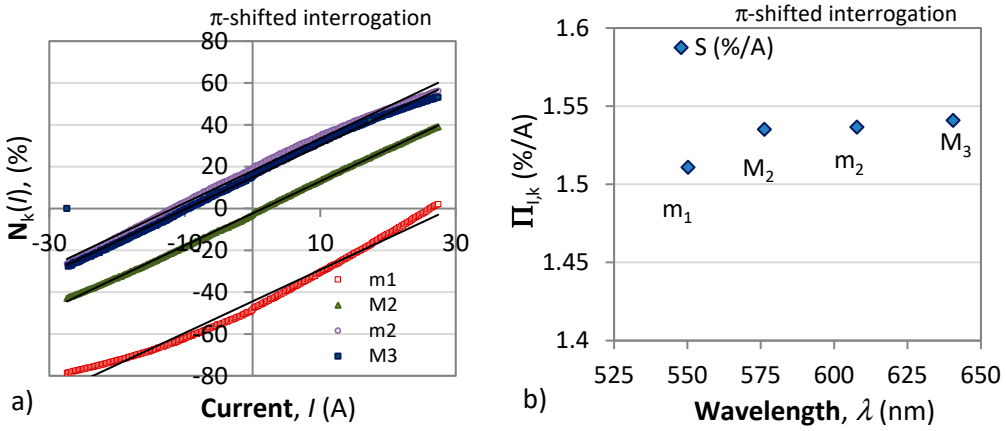


**Figure 5.** Normalized differential responses of the π-shifted interrogation technique: a) wavelength shifts of the the maxima $M_1$, $M_2$, $M_3$ and the minima $m_1$ and $m_2$, b) wavelength dependence of the sensitivities $\Pi_I(\lambda)$ around maxima $M_2$, $M_3$ and minima $m_1$ and $m_2$.

## 3. Experiment and results

### *3.1. Experimental set-up*

To study the possibility for temperatur corrected current measurements we need to know the dependences of the optical activity and the Verdet constant on the wavelength $\rho(\lambda)$, $V(\lambda)$ and on temperature $\rho(T)$, $V(T)$. The experimental set up used to perform the needed measurements is shown in Figure 6.

The light source is a white halogen lamp (Ocean Optics) and the spectrometer was an Avantes VASPEC-ULS2048CL-EVO, (0.5 nm resolution and a 400 nm to 900 nm range). The light from the source is coupled to 600 μm large core quartz-polymer lead-in fiber, collimated at its output, polarized by a polarizer through an angle $\theta$, traverses the BSO crystal, passed through an analyzer oriented to an angle $\alpha$, and focused to and same type of a lead-out fiber. Alternatively, for current and temperature measurements the white light halogen lamp was replaced by a white LED. The BSO crystal (4 x 4 x 25) is placed in an aluminum holder and is heated/cooled using a thermoelectroc cooler (TEC). Polarizer was fixed with transmission axis along the horizontal axis of the crystal. Only the analyzer was rotated during measurements of the optical activity and its temperature dependence. The temperature could be varied from -32°C to 62°C. The power supply could provide a current in the range from -30A to +30A (±0.1 A) which fed the solenoid coil to create a homogeneous magnetic filed along the BSO crystal as shown in Figure 6.

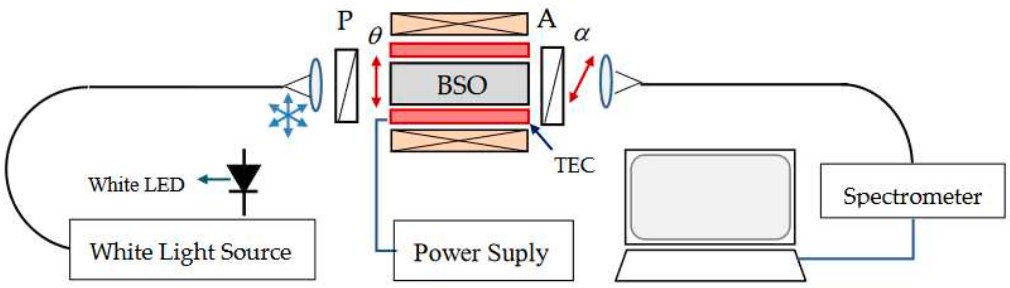


**Figure 6.** Experimental set-up.

### *3.2. Results on optical activity measurements*

Using the set-up shown in Figure 4 we performed a sequence of measurements in which we change the temperature T, current I across the solenoid and measure the output angle of rotation of the polarization at a particular wavelength λ. The measurements were done by compensation of the

Preprints (www.preprints.org) | NOT PEER-REVIEWED | Posted: 17 October 2023 doi:10.20944/preprints202310.1020.v1



polarization rotation via turning the analyzer angle j so that a given minimum at a specified wavelength in the polarimetric response (Figure 2) remains at the same position which means that for a given minimum ($k$ = constant) as

$$\Phi_k = 2\left[\rho(\lambda_k,T)+V_I(\lambda_k,T)I\right]L+2(\theta-\varphi)=(2k+1)\pi \tag{10}$$

The sequence of measurements is as follows:

i) A wavelength among the following 540 nm, 570 nm, 600 nm, 630 nm, 660 nm and 690 nm is chosen starting from the highest value. In the absence of magnetic field ($I$ = 0A) and at room temperature (≈22°C) the analyzer is rotated until a minimum of the response coincides with the chosen wavelength of measurement (690 nm for example).

ii) For a chosen value of the wavelength $\lambda_k$, a value of the current is fixed between $I$ = -30A and $I$ = 30 A. For a fixed value of the current the temperature is varied between $T$ = -30°C to 60°C and for each temperature the analyzer is rotated to compensate for the temperature and current induced phase changes (26) due to the $\rho(\lambda_k,T)$, $V_I(\lambda_k,T)$ and $I$ and the particular value for $\varphi$ is found.

iii) After the temperature is scanned, a new value for the current for the same wavelength is set and then the temperature scanning is repeated.

iv) After all currents are scanned, the next wavelength is chosen and the procedure from i) to iii) is repeated.

The results obtained provide the possibility for the following analysis to be performed. First, the only spectral and temperature dependence is in the optical activity and the Verdet constant and second, neither of them depends on the current, so the compensation angle is represented as.

$$\varphi(\lambda,I,T)=V_I(\lambda,T)L.I+\rho(\lambda,T)L \qquad \text{with} \quad V_I(\lambda,T)I=V(\lambda,T)B \tag{11}$$

Second, we analyze the results for $I$ = 0, which reveal the dependences $\rho(\lambda_k,T)$, so we have

$$\varphi_0(\lambda,T)=\varphi(\lambda,0,T)=\rho(\lambda,T)L \tag{12}$$

Figure 5a) shows a plot of the rotation angle caused by optical activity vs. temperature for the above six wavelengths in the absence of a magnetic field ($I$ = 0). As is seen from this figure, the optical rotation linearly reduces with temperature and can be represented in the form:

$$\varphi_0(\lambda,T)=\rho(\lambda,T)L=\left[a_\rho(\lambda)T+\rho_0(\lambda)\right]L \tag{13}$$

where the thermal coefficient $a_\rho(\lambda)$ that determines the slope of the lines in Figure 5a) as well as the optical activity $\rho_0$ are wavelength dependent.

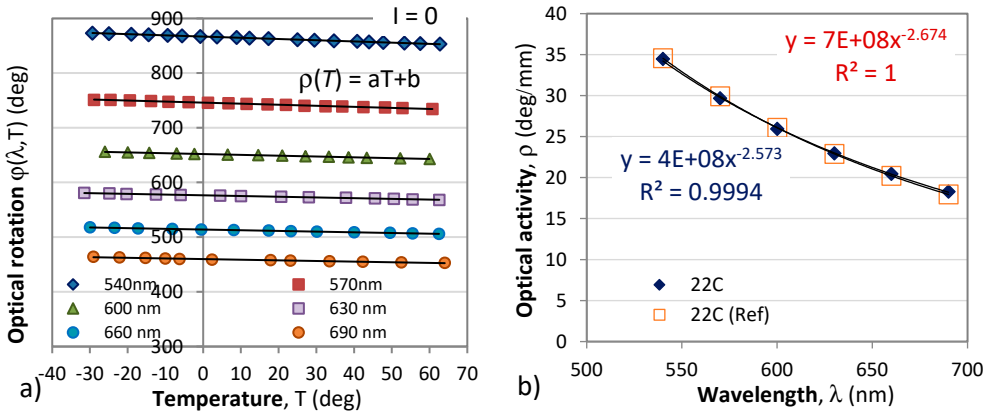

Preprints (www.preprints.org) | NOT PEER-REVIEWED | Posted: 17 October 2023 doi:10.20944/preprints202310.1020.v1



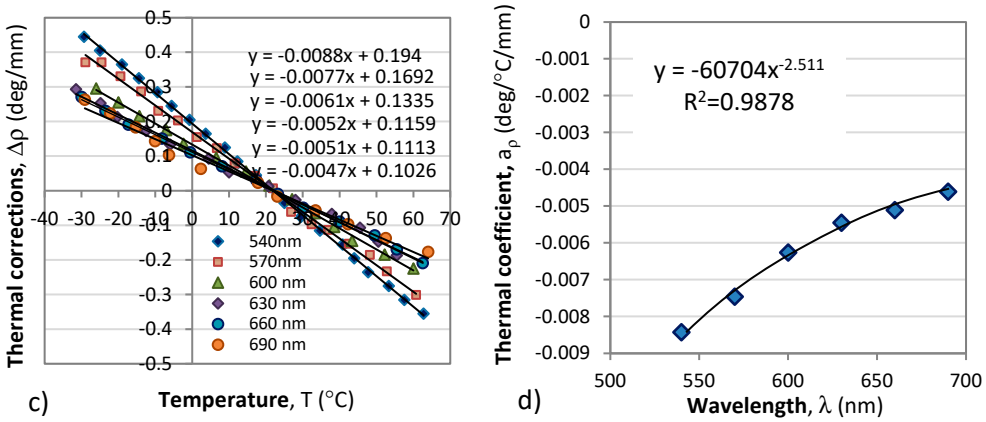


**Figure 7.** Spectral and temperature dependence of the optical rotation without magnetic field ($I = 0$): a) rotation angle vs. temperature at different wavelengths; b) wavelength dependence of the optical activity ρ(λ) at room temperature (22°C); c) temperature corrections Δρ to the optical activity with respect to the response from (b) at room temperature; d) thermal coefficient $a_\rho$.

Third, from the measurements at different temperatures in the -30°C to 60°C range for different currents from -25A to +25A we can retrieve the optical rotation $V_I.L$ (deg/A) due to the magneto-optic effect and its wavelength dependence presented in Figure (8). In that figure we plot $V_I(\lambda).L$ for three temperatures -30°C, 0°C and 60°C and it is seen that the temperature deviations vary randomly in either directions. The relative error due to temperature-dependent deviations of the magneto-optic activity varied with wavelength and on the average was found to be ≈ 0.7%. The relative error due to temperature-dependent deviations of the magneto-optic activity varied with wavelength and on the average was found to be ≈ 0.7 %. We thus conclude that

$$V_I(\lambda,T) = V(\lambda) + \varepsilon(T) \approx V(\lambda) \tag{14}$$

where $\varepsilon(T)$ is a negligible thermally dependent correction

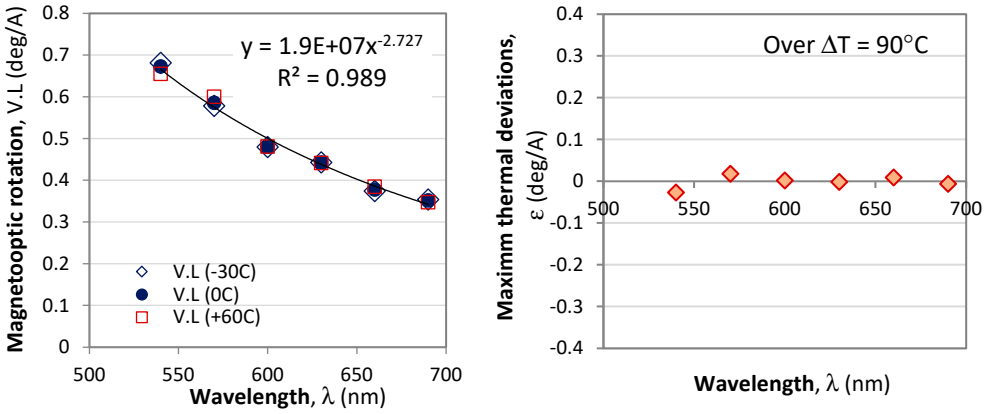


**Figure 8.** Spectral and temperature dependence of the magneto-optical rotation without: a) $V(\lambda)L$; b) the maximum thermally induced variations over a 90°C temperature range.

*3.3. Approximations*

The experimental plots obtained for $\rho_0(\lambda)$, $a_\rho(\lambda)$ and $V(\lambda)$ are found to be sufficiently well approximated by power law functions namely as:

$$\rho_0(\lambda) = R_0\lambda^{-r} \qquad R_0 = 4\text{x}10^8\,,\quad r = -2.573 \quad (R^2 = 0.9995) \tag{15a}$$

$$a_\rho(\lambda) = A_0\lambda^{-a} \qquad A_0 = -\,60704,\ a = -2.511 \quad (R^2 = 0.9878) \tag{15b}$$

Preprints (www.preprints.org) | NOT PEER-REVIEWED | Posted: 17 October 2023 doi:10.20944/preprints202310.1020.v1



$$V_I(\lambda) = V_0\lambda^{-v} \qquad V_0 = 760533,\ v = -2.728 \quad (R^2 = 0.9896) \tag{15c}$$

Based on the above we can write (14) as

$$\varphi(\lambda, I, T) = \rho(\lambda, T)L + V_I(\lambda)L.I = a_\rho(\lambda)T.L + \rho_0(\lambda).L + V_I(\lambda)I.L \tag{16a}$$

and for λ from 540 nm to 700 nm and $T$ from -30°C to +60°C the power law approximations (31) can be used for all wavelength dependences:

$$\varphi(\lambda, I, T) = \left[A_0\lambda^{-a}T + R_0\lambda^{-r} + V_0\lambda^{-v}..I\right]L \tag{16b}$$

## 4. Simultaneous current and temperature measurement technique

### *4.1. Sensitivities to current and temperature*

To realize temperature corrected current measurement the non-linear power-law approximations for $a_\rho(\lambda)$, $\rho_0(\lambda)$ and $V(\lambda)$ are simplified according to the following procedure:

i) Use the power law approximations (31) to study the responses to current and temperature changes and determine the sensitivities $S_I$ and $S_T$.
ii) Study the wavelength, temperature and current (magnetic field) dependences of $S_I$ and $S_T$.
iii) Develop a method for simultaneous two parameter measurement.

We first model the white light LED spectral distribution used in the sensor by a shifted Gamma function defined as [31]:

$$S(\lambda) = \frac{\beta^\alpha}{\Gamma(\alpha)}(\lambda - \lambda_0)^{-\alpha} e^{-\beta(\lambda-\lambda_0)} \tag{17}$$

Taking into account (31) and (32), the intensity distribution at the analyzer can be represented as

$$I(\lambda, I, T) = \frac{I_0}{4}S(\lambda)\left\{1 + \cos\left[\left(A_0\lambda^{-a}T + R_0\lambda^{-r} + V_0\lambda^{-v}.I\right)L + 2(\theta - \varphi)\right]\right\} \tag{18}$$

The parameters for the Gamma function are as follows: $\lambda_0$ = 515 nm, $\alpha$ = 3.75 and $\beta$ = 27. The theoretical fit using (17) a real polarimetric responses at analyzer angle 0° is presented in Figure 7 and is compared to the response at 60°.

The full differential of the phase per unit length dΦ/2L is found from (3b)

$$\frac{d\Phi}{2L} = \left(-aA_0\lambda^{-a-1}T - rR_0\lambda^{-r-1} - vV_0\lambda^{-v-1}.I\right)d\lambda + \left(-vV_0\lambda^{-v-1}\right)dI + \left(A_0\lambda^{-a}\right)dT \tag{19a}$$

$$\frac{d\Phi}{2L} = F_\lambda d\lambda + F_I dI + F_T dT \tag{19b}$$

In case of spectral interrogation by extremum tracking $d\Phi$=0 and we find for $\delta\lambda$ as

$$d\lambda = -\frac{F_I}{F_\gamma}dI - \frac{F_T}{F_\lambda}dT = S_I dI + S_T dT \tag{20a}$$

$$S_I = \frac{d\lambda}{dI} = -\frac{F_I}{F_\gamma}, \qquad S_T = \frac{d\lambda}{dT} = -\frac{F_T}{F_\gamma} \tag{20b}$$

As the power law expressions are nonlinear we proceed to the second step outlined above and perform a study of the wavelength, temperature and current (magnetic field) dependences of $S_I(\lambda, I, T)$ and $S_T(\lambda, I, T)$. To do that we change the current $I$ at a constant temperature $T$, and then change temperature for constant current and measure the resulting wavelength shifts of the minima and

Preprints (www.preprints.org) | NOT PEER-REVIEWED | Posted: 17 October 2023 doi:10.20944/preprints202310.1020.v1



maxima in the distribution from Figure 9. The we plot the dependence of $\Delta\lambda$ vs $I$ for different temperatures for each extremum, as well as $\Delta\lambda$ vs $T$ for different currents, from which we determine the needed sensitivities.

$$\Delta\lambda = S_I(\lambda,T)\Delta I + S_T(\lambda,I)\Delta T \tag{21}$$

Figure 10 shows the wavelength changes of four minima

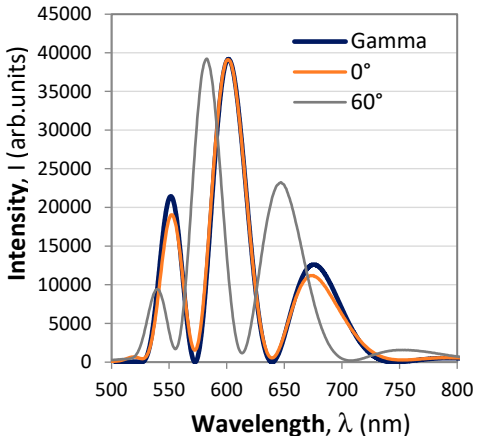


**Figure 9.** Two responses of the polarimetric sensor for the analyzer turned at 0° and 90° given by the thin line. The thick line is a theoretical fitting to the response at 0° from (18).

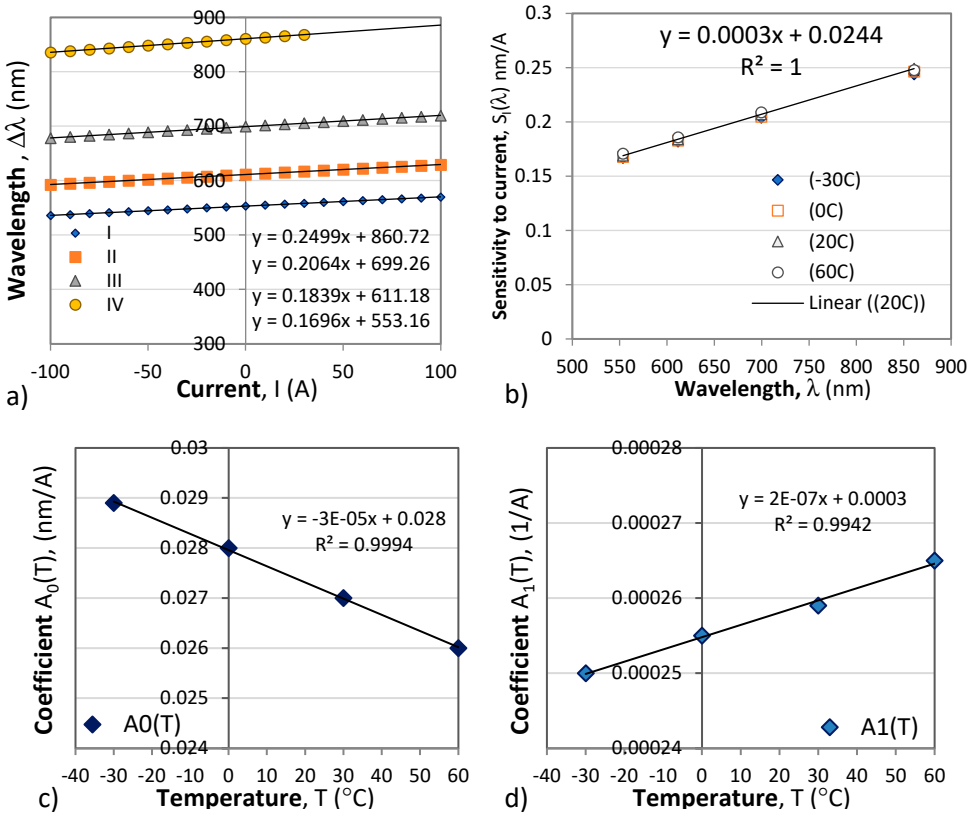


**Figure 10.** Responses to current changes: s) shifts of the extremun wavelength vs. current changes from -100 A to 100 A; b) wavelength dependence of the sensitivity to current $S_I(\lambda)$; c) the temperature dependence of the coefficient $A_0(T)$ from (22a); d) the temperature coefficient $A_1(T)$.

The wavelength dependence for the current sensitivity $S_I(\lambda)$ is experimentally confirmed in ref [31] and as we see at each wavelength the $\Delta\lambda(I)$ dependence is linear. So is the $S_I(\lambda)$ over the range of wavelengths above 550 nm, though weakly dependent on temperature.

Preprints (www.preprints.org) | NOT PEER-REVIEWED | Posted: 17 October 2023 doi:10.20944/preprints202310.1020.v1



As is seen from Figure 10b) the sensitivity to current is linearly dependent on the wavelength and can be repres4nted as follows

$$S_I(\lambda) = A_0(T) + A_1(T)\lambda \qquad \text{(nm/A)} \tag{22a}$$

The linear fits of each of the coefficients presented in Figure 10c) and 10d) below can be represented as follows:

$$A_0(T) = A_{00} + A_{01}T \quad \text{(nm/A)} \qquad \text{and} \qquad A_1(T) = A_{10} + A_{11}T \qquad \text{(1/A)} \tag{22b}$$

The wavelength shifts of the four minima with temperature and the temperature sensitivity on the wavelength $S_T(\lambda)$ at different current levels is presented in Figure 11.

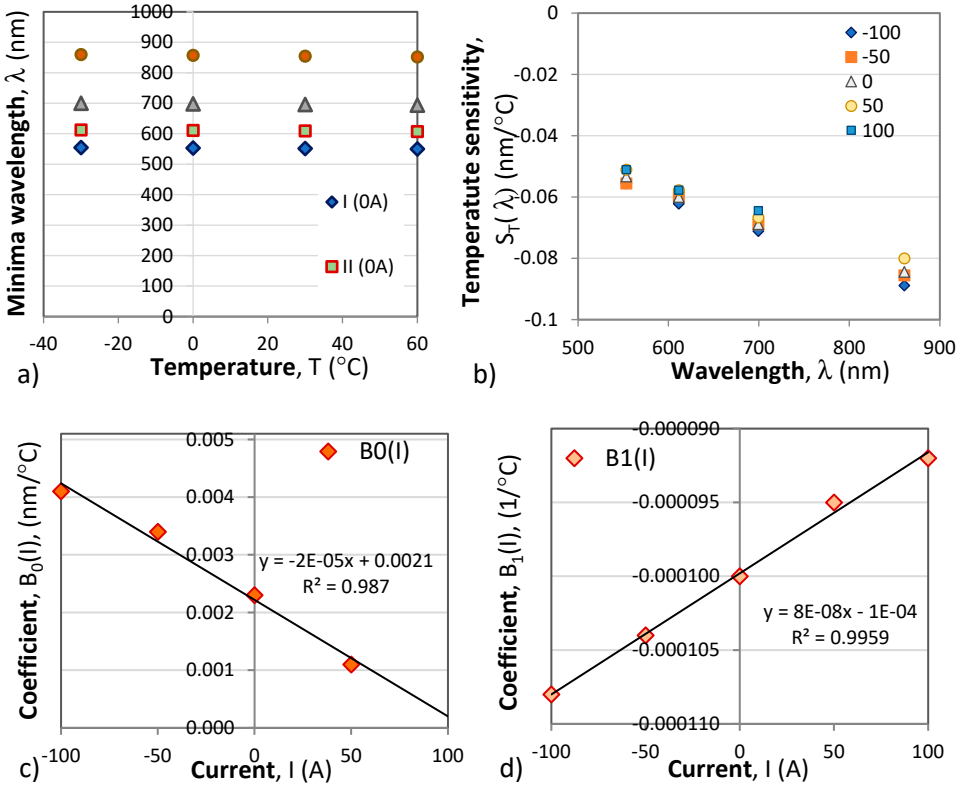


**Figure 11.** Temperature dependence: a) Temperature induced wavelength shifts of four minima at I = 0A; b) Wavelength dependence of sensitivities to temperature $S_T(\lambda)$ for different currents; c) temperature dependence of the B0 coefficient from (23a); the thermal coefficient $B_1$from (23).

From Figure 9 b) it is seen that the temperature sensitivity $S_T(\lambda,I)$ is linearly dependent on the wavelength and can be written as:

$$S_T(\lambda, I) = B_0(I) + B_1(I)\lambda \qquad \text{(nm/°C)} \tag{23a}$$

where the $B_0(I)$ and $B_1(I)$ are also linear functions of the current Figure 9c) and 9d) and are written as:

$$B_0(I) = B_{00} + B_{01}I \quad \text{(nm/°C) and} \qquad B_1(T) = B_{10} + B_{11}I \qquad \text{(1/°C)} \tag{23b}$$

As follows from (21)

$$\lambda - \lambda_0 = S_I(\lambda,T)(I - I_0) + S_T(\lambda,I)(T - T_0)$$

Preprints (www.preprints.org) | NOT PEER-REVIEWED | Posted: 17 October 2023 doi:10.20944/preprints202310.1020.v1



*4.2. Two points method for simultaneous two-parameter measurement*

In this form the unknown quantities are the current $I$ and temperature $T$ and after insertion of (22b) into (22a) and of (23b) into (23a) we obtain after some rework for the k-th extremum tracked we can write

$$\lambda_k - \lambda_{k0} = \Delta\lambda_k = A_k \Delta I + B_k \Delta T + C_k \Delta I \Delta T \tag{24}$$

Where

$$A_k = A_{00} + A_{10}\lambda_k - A'_k T_0 \qquad A'_k = A_{01} + A_{11}\lambda_k \tag{25a}$$

$$B_k = B_{00} + B_{10}\lambda_k - B'_k I_0 \qquad B'_k = B_{01} + B_{11}\lambda_k \tag{25b}$$

$$C_k = A'_k + B'_k \tag{25c}$$

Equation (24) contains a mixed term proportional to $\Delta I \Delta T$. To eliminate the temperature dependence we chose two extrema wavelengths choose $\lambda_1$ and $\lambda_2$ ($k$ = 1, 2) to track to our choice. By varying the orientation of the analyzer we can fine tune the position of the pattern. Eq. (24) then is written for each of the wavelengths as:

$$\Delta\lambda_1 = A_1 \Delta I + B_1 \Delta T + C_1 \Delta I \Delta T \tag{26a}$$

$$\Delta\lambda_2 = A_2 \Delta I + B_2 \Delta T + C_2 \Delta I \Delta T \tag{26b}$$

Solving (26a,b) with respect to the mixed ΔT term and eliminating the temperature dependence leads to a quadratic equation with respect to the current:

$$a\Delta I^2 + b\Delta I + c = 0 \tag{27}$$

**W**here

$$a = A_1 C_2 - C_1 A_2, \qquad b = \Delta\lambda_2 C_1 - \Delta\lambda_1 C_2 + A_1 B_2 - B_1 A_2, \qquad c = \Delta\lambda_2 B_1 - \Delta\lambda_1 B_2 \tag{28}$$

Solving (37) with respect to ΔI yields

$$\Delta I = \frac{-b - \sqrt{b^2 - 4ac}}{2a} \tag{29}$$

The electric current measurement procedure runs thus as follows:

i) The coefficients from Table 1 are substituted in (25).
ii) By fixing the position of the analyzer with respect to the polarizer, a desirable position of the spectral response is fixed for $I_0$=0 and $T = T_0$ which quantities are also to be inserted in (35). The two extrema whose shifts are to be monitored are fixed and under these conditions their values $\lambda_{10}$ and $\lambda_{20}$ are measured and substituted in (25) as well.
iii) The instant values of the extrema $\lambda_1$ and $\lambda_2$ are measured over regular intervals $\Delta t$ are inserted into (25) and into (28) for the coefficients $a$, $b$ and $c$ from (27)
iv) The current change is calculated (29).

**Table 1.** Coefficients for the expressions for the sensitivities $S_I$ and $S_T$.

| $A_{00}$ (nm/A) | $A_{01}$ (nm/°C/A) | $A_{10}$ (1/A) | $A_{11}$ (1/°C/A) | $B_{00}$ (nm/°C) | $B_{01}$ (nm/°C/A) | $B_{10}$ (1/°C) | $B_{11}$ (1/°C/A) |
|---|---|---|---|---|---|---|---|
| $2.8\times10^{-02}$ | $-3\times10^{-5}$ | $2{,}548\times10^{-4}$ | $2\times10^{-7}$ | $2.1\times10^{-3}$ | $-2.05\times10^{-5}$ | $-9.97\times10^{-5}$ | $8.2\times10^{-8}$ |

To test the method we perform the above procedure by setting in (29) the current $I$ from -100A to +100 A for temperatures $T$= -30C, 0C, 30C, 60C and 90C which causes the spectral response to shift. For each combination of current and temperature we determine the values of the wavelengths $\lambda_1$, $\lambda_2$

Preprints (www.preprints.org) | NOT PEER-REVIEWED | Posted: 17 October 2023 doi:10.20944/preprints202310.1020.v1



and $\lambda_3$ of the three observable minima which values are inserted into (25). The reference wavelength values $\lambda_{1,0}$ = 525.7nm, $\lambda_{2,0}$ = 572.8 nm and $\lambda_{3,0}$ = 639.7 nm from (34) are at $T_0 = 0$ and $I_0 = 0$. The pairs of wavelengths to determine the current are ($\lambda_1$, $\lambda_3$) and ($\lambda_2$, $\lambda_3$). Figure 9 shows the correspondence between the preset value of the current $I$ and the calculated $I_c$ for each of the pairs from equation (29). The results obtained for the temperatures from -30C to +90C reveal that the correspondence is linear and close to an identity function, yet from the linear fits the proportionality coefficient is 0.9438 for the first pair and 0.9316 for the second (Figure 10a,b). We first note that on the average the responses are the same for all temperatures. Second, a certain non-linearity is observed and third, the two correspondences are differently offset from the origin of the coordinate system. Figure 13a) show the correspondences averaged over all temperatures with a third degree polynomial. Figure 13b) shows the average of the two responses form Figure 13a).

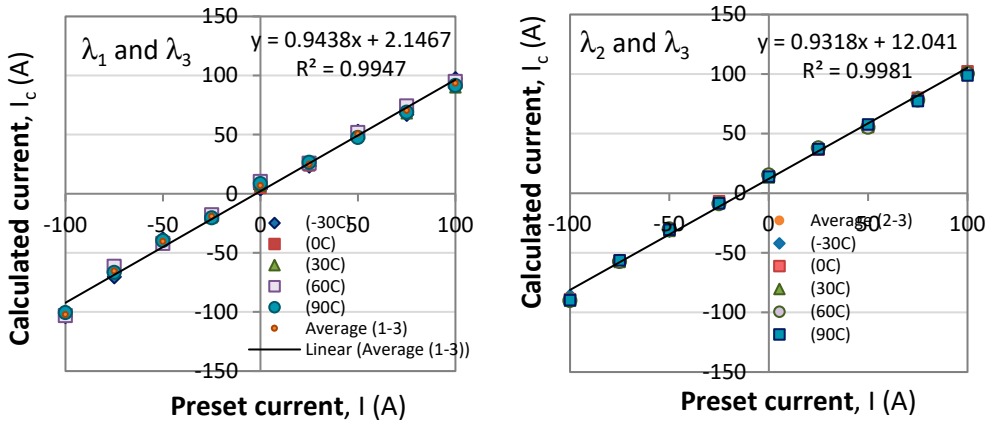


**Figure 12.** Correspondence between calculated current and preset current: a) for the ($\lambda_1$, $\lambda_3$) pair; b) for the ($\lambda_2$, $\lambda_3$) pair.

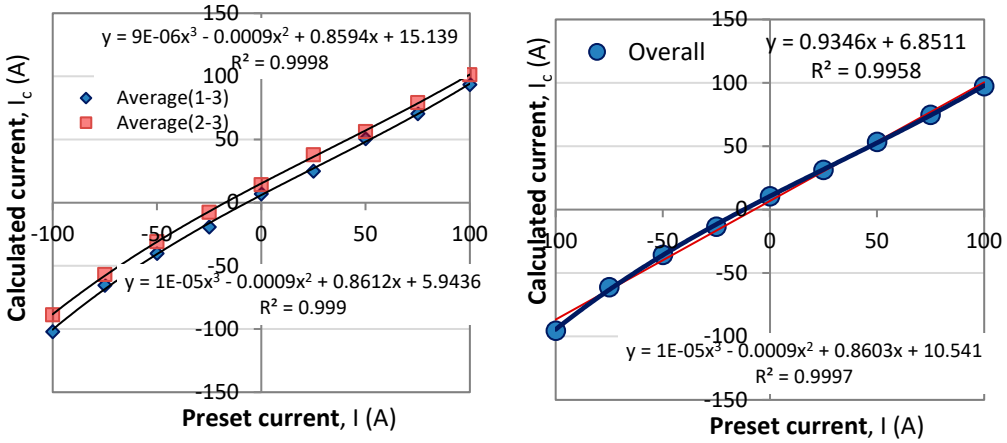


**Figure 13.** Correspondence between calculated current and preset current: a) for the ($\lambda_1$, $\lambda_3$) pair; b) for the ($\lambda_2$, $\lambda_3$) pair.

**Table 2.** Coefficients of the linear and third order polynomial fits for the correspondence plots of the calculated $I_c$ versus preset value of the current $I$.

| Pairs | Linear | Third degree polynomial |
|---|---|---|
| ($\lambda_1$, $\lambda_3$) | $I_c = 0.9438\ I + 2.1467$ ($R^2$=0.9947) | $I_c = 1.10^{-5}\ I^3 - 0.0009\ I^2 + 0.8612 + 5.9436$ ($R^2$=0.999) |
| ($\lambda_2$, $\lambda_3$) | $I_c = 0.9318\ I + 12.041$ ($R^2$=0.9981) | $I_c = 9.10^{-6}\ I^3 - 0.0009\ I^2 + 0.8594 + 15.139$ ($R^2$=0.9947) |
| Overall | $I_c = 0.9346\ I + 6.8511$ ($R^2$=0.9958) | $I_c = 1.10^{-5}\ I^3 - 0.0009\ I^2 + 0.8603 + 6.8511$ ($R^2$=0.9997) |

 doi:10.20944/preprints202310.1020.v1



Figures 12 and 13 reveal that the slight nonlinearity is observed at the extremities for negative currents. These we assume are due to the neglect of the weak temperature dependence of the Verdet constant from Figure 8b and to extending by a factor of more than three the current range in the simulations compared to the range of measurements to determine the sensitivities. The high values of the coefficient of determination $R^2$ for the third order polynomial mean that a convenient look-up table can be compiled to list the correct value of the preset current.

## 4. Conclusions

The performed measurements, subsequent analysis and simulations of a polarimetric current sensor with spectral interrogation allow us to formulate the following conclusions:

1. Two types of spectral interrogation techniques could be used: wavelength shifts of the minima and/or maxima and normalized differential intensity response at pairs of wavelengths which are $\pi$-shifted over the spectral range. In both cases the sensitivities to current are wavelength dependent.
2. We have performed detailed measurements on the temperature, current and spectral dependences of the intrinsic and magnetic field induced optical activity of BSO crystals in the range from 540 nm to 690 nm, current range from -30 to +30 A and temperature range from -30C to 60 C.
3. The temperature dependence of the intrinsic optical activity $\rho(\lambda,T)$ was found to be linear in the form $\rho(\lambda,T) = \rho_0(\lambda)+a(\lambda)T$ within the above range while the wavelength dependence of the coefficients $\rho_0(\lambda)$ and $a_\rho(\lambda)$ could be fitted with a coefficients of determination of $R^2$=0.9878 or better.
4. The temperature dependence of the Verdet constant was found to be very weak and over a $\Delta T$ = 90°C temperature range is less than $1.08\text{x}10^{-3}$ deg/A/mm, typically $<7.2\text{x}10^{-4}$ deg/A/mm above 570 nm. The wavelength dependence of the Verdet constant could be fitted by a power law with $R^2$=0.989.
5. On the basis of the above established approximations it has been found that the wavelength shift of an extremum is a linear combination of the current and temperature changes but contains a mixed term. By making use of spectral shifts at two extrema $\lambda_1$ and $\lambda_2$, the temperature dependence is lifted and a second order polynomial equation for current changes $\Delta I$ has been derived.
6. A straightforward current measurement procedure has been proposed and tested numerically.

**Author Contributions:** T. E. – conceptualization, investigation, formal analysis, writing of the manuscript, funding, G. D. – conceptualization, methodology, investigation, supervision, funding, P.K. – data curation, investigation, resources, V.V. – investigation, resources.

**Funding:** This research was funded by the Bulgarian National Science Fund, grant number KP-06-N48/2 entitled "Spectral polarimetry of polarized fluorescence in magneto-optical materials and its application to precision magnetic field sensors".

**Conflicts of Interest:** The authors declare no conflict of interest.

## References

1. J. Zhang, C. Wang, Y. Chen, Y. Xiang, T. Huang, P. P. Shum, Z. Wu, "Fiber structures and material science in optical fiber magnetic field sensors" Frontiers of Optoelectronics (2022) 15:34
2. K. Bohnert, P. Gabus, J. Kostovic, H. Brändle, "Optical fiber sensors for the electric power industry," Optics and Lasers in Engineering, **43** ( 3–5), 511-526 (2005).
3. W. Leysen, A. Gusarov, M. Wuilpart, P. Beaumont, A. Boboc, D. Croft, N. Bekris, P. Batistoni, "Plasma current measurement at JET using polarimetry-based fibre optic current sensor," Fusion Engineering and Design, **160**, 111754 (2020).
4. P.Mihailovic and S. Petricevic, "Fiber Optic Sensors Based on the Faraday Effect," Review, Sensors, **21**, 6564, (2021).

5. C. Liu, T. Shen, H.-B. Wu, Y. Feng , J.-J. Chen, "Applications of magneto-strictive, magneto-optical, magnetic fluid materials in optical fiber current sensors and optical fiber magnetic field sensors: A review," Optical Fiber Technology, **65**, 102634, (2021).
6. J. Peng, S.Zhang, S.Jia, X. Kang, H. Yu, S. Yang, S. Wang, Y. Yang, "A highly sensitive magnetic field sensor based on FBG and magnetostrictive composite with oriented magnetic domains," Measurement **189**, 110667, (2022).
7. H. Zhang, Z. Xie, H. Yan, P. Li, P.Wang, D. Han, "High sensitivity and large measurement range magnetic field micro-nano fiber sensor based on Mach-Zehnder interference," Optics & Laser Techn. **156**, 108455, (2022).
8. C. Shuhao, M. Sergeev, A. Petrov, S. Varzhel, C. Sheng, L. Li, "Highly sensitive vector magnetic field sensors based on fiber Mach–Zehnder interferometers, Optics Communications **524**, 128725, (2022).
9. X.Wang, Y. Zhao, R.Lv, H.Zheng, "Optic-fiber vector magnetic field sensor utilizing magneto-shape effect of magnetic fluid," Measurement **202**, 111829, (2022).
10. N. Alberto, M. F. Domingues, C. Marques, P. André and P. Antunes, Optical Fiber Magnetic Field Sensors Based on Magnetic Fluid: A Review , 2018, Sensors 18(12): 4325
11. X. Li, Q. Yu, X. Zhou, Y. Zhang, R. Lv, Y. Zhao, "Magnetic sensing technology of fiber optic interferometer based on magnetic fluid: A review", Measurement, Vol. 216, 2023, 112929
12. V. Tassev, M. Gospodinov, M. Veleva, "Optical activity of BSO crystals doped with Cr, Mn and Cu," Optical Materials **13**, 249-253 (1999).
13. V. Tassev, G. Diankov and M. Gospodinov, "Measurement of optical activity and Faraday effect in pure and doped sillenite crystals," SPIE **2529**, 223-230 (1995).
14. G. L. Diankov, V. L. Tassev, M. Gospodinov, "Fiber optic magnetic field sensor head based on BSO crystal," Proc. SPIE **3052**, Ninth Int. School on Quantum Electronics: Lasers--Physics and Applications, (27 Dec. 1996).
15. L. Wang, Y. Huang, C. Deng, C. Hu, and T. Wang, A Compact Polarimetric Fiber-optic Sensor Based on $Bi_4Ge_3O_{12}$ Crystal for Ultra-high Surge Current Sensing, Optical Fiber Sensors 2018, Lausanne Switzerland, 24–28 September 2018, ISBN: 978-1-943580-50-
16. M. Isik, S. Delice, N. M. Gasanly, N. H. Darvishov, and V. E. Bagiev, "Temperature-dependent band gap characteristics of $Bi_{12}SiO_{20}$ single crystals," J. Appl. Phys. **126**, 245703 (2019).
17. P. Mihailovic, S. Petricevic, S. Stankovic, J. Radunovic, "Temperature dependence of the $Bi_{12}GeO_{20}$ optical activity," Optical Materials **30**, 1079–1082 (2008)
18. F. Lessmann and F. Jenau, "Temperature Compensation Method for an Optical Direct Current Sensor Using Two Wavelengths and Technical Current Ripple," 2018 IEEE Int. Conf. on Environment and Electrical Engineering and 2018 IEEE Industrial and Commercial Power Systems Europe (EEEIC / I&CPS Europe), 1-4 (2018).
19. P. M. Mihailovic, S. J. Petricevic and J. B. Radunovic, "Compensation for Temperature-Dependence of the Faraday Effect by Optical Activity Temperature Shift," in IEEE Sensors Journal **13** (2) 832-837, (2013).
20. H. Zhao, F. Sun, Y. Yang, G. Cao, K. Sun, "A novel temperature-compensated method for FBG-GMM current sensor," Optics Communications, **308**, 64-69 (2013).
21. Q. Yu, X.-G. Li, X. Zhou, N. Chen, S. Wang , F. Li, R.-Q. Lv, L. V. Nguyen, S. C. Warren-Smith and Y. Zhao, "Temperature Compensated Magnetic Field Sensor Using Magnetic Fluid Filled Exposed Core Microstructure Fiber," in IEEE Transactions on Instrumentation and Measurement, **71**, 1-8, (2022), Art no. 7004408
22. X.Wang, R. Lv, Y. Zhao, J. Zhao, Z.Lin, "Temperature-compensated optical fiber magnetic field sensor with cascaded femtosecond laser micromachining hollow core fiber and fiber loop," Optics & Laser Technology, **157**, 108748, (2023).
23. Y. Zhou, X. Liu, L. Fan, W. Liu, E. Xing, J. Tang, J. Liu, "Temperature and vibration insensitive fiber optic vector magnetic field sensor," Optics Communications, 129178, (2022).
24. D. Reilly, A. J. Willshire, G. Fusiek, P. Niewczas and J. R. McDonald, "A Fiber-Bragg-Grating-Based Sensor for Simultaneous AC Current and Temperature Measurement," IEEE Sensors Journal, **6** (6) 1539-1542, (2006).
25. C. Li, T. Ning, X. Wen, J. Li, C. Zhang, C. Zhang, "Magnetic field and temperature sensor based on a no-core fiber combined with a fiber Bragg grating," Optics & Laser Technology, **72**, 104-107 (2015).
26. G. -H. Su, J. Shi, D.-G. Xu, H.-W. Zhang, W. Xu, Y.-Y. Wang, J.-C. Feng and J.-Q. Yao, "Simultaneous Magnetic Field and Temperature Measurement Based on No-Core Fiber Coated With Magnetic Fluid," IEEE Sensors Journal, **16** (23). 8489-8493 (2016).
27. C. Sun, M. Wang, Y. Dong, S. Ye, S. Jian, "Simultaneous measurement of magnetic field and temperature based on NCF cascaded with ECSF in fiber loop mirror," Optical Fiber Technology, **48**, 45-49, (2019).
28. R.Xu, Y.Xue, M.Xue, C.Ke, J.Ye, M.Chen, H.Liu, L.Yuan, "Simultaneous Measurement of Magnetic Field and Temperature Utilizing Magnetofluid-Coated SMF-UHCF-SMF Fiber Structur," Materials **15**, 7966 (2022).

29. Y. Huang, H. Qiu, C. Deng, Z. Lian, Y. Yang, Y. Yu, C. Hu, Y. Dong, Y. Shang, X. Zhang, and T.Wang, "Simultaneous measurement of magnetic field and temperature based on two anti-resonant modes in hollow core Bragg fiber," Opt. Express **29**, 32208-32219 (2021)
30. T. Eftimov, G. Dyankov, P. Kolev, V.Vladev, L. Kolaklieva, "A polarimetric fiber optic current sensor based on Bi12SiO20 crystal fluorescence," Optical Materials, **133**, 112837 (2022).
31. T.Eftimov, G.Dyankov, P. Kolev, V.Vladev, "A simple fiber optic magnetic field and current sensor with spectral interrogation," Optics Communications," **527**, 128930 (2023).
32. R. B. Lauer, "Photoluminescence in $Bi_{12}SiO_{20}$ and $Bi_{12}GeO_{20}$," Appl. Phys. Lett. **17**, 178 (1970).
33. T. Eftimov, G.Dyankov, A. Arapova, P. Kolev And V. Vladev, "Temperature stability of a polarimetric current sensor based on BSO crystal fluorescence," W4.73, OFS-27, Optical Fiber Sensor Conference – 2022, 29 Aug- 2 Sept., The Westin Alexandria, Alexandria, Virginia, USA